# Zinc Ion Effects on Individual *Ssp* DnaE Intein Splicing Steps: Regulating Pathway Progression

Nicole Magnasco Nichols, Jack S. Benner, Deana D. Martin, and Thomas C. Evans, Jr.*

*New England Biolabs, Inc., Beverly, Massachusetts 01915-5599*

*Received November 27, 2002; Revised Manuscript Received March 7, 2003*

ABSTRACT: Use of the naturally split, self-splicing *Synechocystis* sp. PCC6803 DnaE intein permits separate purification of the N- and C-terminal intein domains. Otherwise spontaneous intein-mediated reactions can therefore be controlled in vitro, allowing detailed study of intein kinetics. Incubation of the *Ssp* DnaE intein with $ZnCl_2$ inhibited trans splicing, hydrolysis-mediated N-terminal trans cleavage, and C-terminal trans cleavage reactions. Maximum inhibition of the splicing reaction was achieved at equal molar concentrations of $ZnCl_2$ and intein domains, suggesting a 1:1 metal ion:intein binding stoichiometry. Mutation of the $^{+}1$ cysteine residue to valine ($C^{+}1V$) alleviated the inhibitory effects of $ZnCl_2$. Valine substitution in the absence of $ZnCl_2$ blocked trans splicing and decreased C-terminal cleavage kinetics in a manner similar to that of the native $^{+}1$ cysteine in the presence of $ZnCl_2$. These data are consistent with $Zn^{2+}$-mediated inhibition of the *Ssp* DnaE intein via chelation of the $^{+}1$ cysteine residue. N-Terminal trans cleavage can occur via both spontaneous hydrolysis and nucleophilic (e.g., DTT) attack. Comparative examination of N-terminal cleavage rates using amino acid substitution ($C^{+}1V$) and $Zn^{2+}$-mediated inhibition permitted the maximum contribution of hydrolysis to overall N-terminal cleavage kinetics to be determined. Stable intermediates consisting of the associated intein domains were detected by PAGE and provided evidence of a rapid C-terminal cleavage step. Acute control of the C-terminal reaction was achieved by the rapid reversal of $Zn^{2+}$-mediated inhibition by EDTA. By inhibiting both the splicing pathway and spontaneous hydrolysis with $Zn^{2+}$, reactants can be diverted from the trans splicing to the trans cleavage pathway where DTT and EDTA can regulate N- and C-terminal cleavage, respectively.

Inteins (*1*) are protein segments capable of self-excision from flanking protein sequences termed exteins (reviewed in refs *2* and *3*). Intein-mediated splicing results in ligation of two previously interrupted extein sequences into a single polypeptide chain and requires no additional cofactors or proteins (*4*, *5*). First described in 1990 (*6*, *7*), inteins have now been identified in archaeal, bacterial, and eukaryotic organisms and range in size from 134 to 608 amino acid residues (compiled in InBase, the Intein Database, at New England Biolabs, http://www.neb.com/neb/inteins.html) (*8*). The majority of inteins contain an internal homing endonuclease domain that is believed to mediate horizontal gene transfer (reviewed in refs *9*−*11*). This domain is not required for splicing activity by either naturally occurring or genetically engineered mini-inteins (*12*−*17*).

Examination of intein-mediated reactions is complicated by their spontaneous nature. In vitro, use of the naturally split *Synechocystis* sp. PCC6803 DnaE mini-intein (*Ssp* DnaE intein) allows the starting point of the reaction to be closely regulated (*13*, *18*). The coding sequence for the *Ssp* DnaE intein is found in the split catalytic subunit of the DNA polymerase III gene (*dnaE*), whose two genes are located 745 kb apart in the native genome (*19*, *20*). In *Synechocystis* sp., the intein is believed to generate full-length, active DnaE protein via trans splicing, although direct evidence has not been presented. Both trans and cis splicing activities (from the two separate intein domains and the fused domains, respectively) have been demonstrated for the *Ssp* DnaE intein in vitro as well as in *Escherichia coli* (*13*, *19*).

In addition to trans splicing, the *Ssp* DnaE intein can facilitate peptide bond cleavage at either the N- or C-terminal junction of the intein−extein sequence (Figure 1). For this intein, cleavage appears to progress in a linear pathway, with N-terminal cleavage being a prerequisite for C-terminal cleavage. The process of N-terminal cleavage, although spontaneous, can be enhanced in vitro by the addition of reagents such as DTT,[1] HA, and MESNA (*21*−*23*). Although these nucleophiles are known to induce N-terminal cleavage via attack of the linear thioester intermediate (Figure 1, reaction III), progression of the spontaneous process has not been uniquely defined and likely occurs via hydrolysis of either the linear or branched thioester intermediates.

The mechanism of intein splicing has been studied and reviewed in detail (*3*, *21*, *22*, *24*). Amino acid residues typically required for splicing activity are conserved and have been mapped mainly to the junction of the intein−extein sequence. As demonstrated by X-ray crystallographic studies, the two termini of an intein fold into a single active site, bringing these amino acids close together (*25*−*27*). In

* To whom correspondence should be addressed: New England Biolabs, Inc., 32 Tozer Rd., Beverly, MA 01915. Telephone: (978) 927-5054. Fax: (978) 921-1350. E-mail: evans@neb.com.

[1] Abbreviations: Ab, antibody; DTT, 1,4-dithio-DL-threitol; EDTA, ethylenediaminetetraacetic acid; HA, hydroxylamine hydrochloride; HRP, horseradish peroxidase; IPTG, isopropyl $\beta$-D-thiogalactopyranoside; LB, Luria-Burtani broth; MESNA, sodium 2-mercaptoethanesulfonate; TCEP, tris(2-carboxyethyl)phosphine hydrochloride; PVDF, polyvinylidene fluoride.

10.1021/bi020679e CCC: $25.00 
Published on Web 04/18/2003

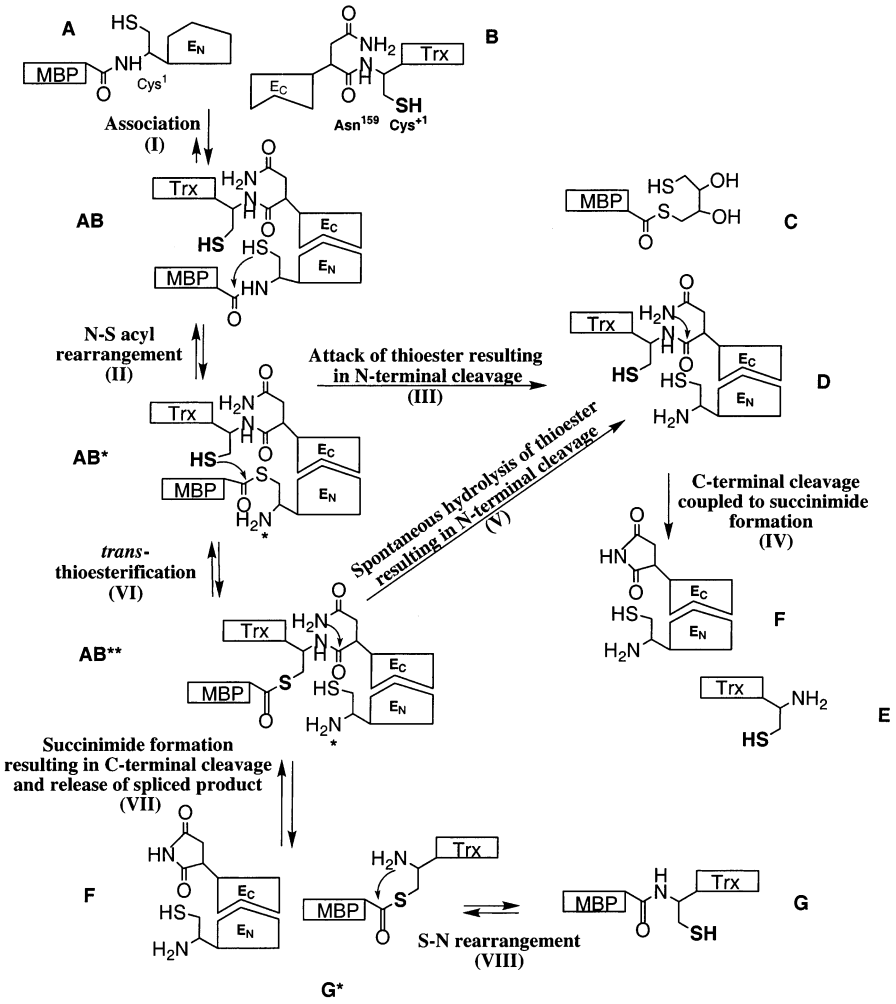


FIGURE 1: Mechanism of *Ssp* DnaE trans splicing and trans cleavage. Association of the two intein domains (I) has been demonstrated to be rapid relative to the overall rate of splicing and cleavage reactions. Rearrangement of the N-terminal scissile bond (II) yields a reactive thioester that can be attacked by nucleophilic reagents such as DTT, HA, and MESNA, leading to N-terminal cleavage (III). Cyclization of the C-terminal asparagine residue (N159) results in C-terminal cleavage (IV). Trans splicing occurs in vitro in the absence of an exogenous nucleophile, with attack of the N-terminal thioester by the $^{+}1$ cysteine residue (bold) yielding a branched thioester intermediate (VI). Cyclization of N159 results in peptide bond cleavage, liberating the associated extein domains from the intein halves (VII). The ligated exteins undergo a final S−N rearrangement, uncatalyzed by the intein, to yield a single polypeptide chain (VIII). Note that trans cleavage does not involve extein ligation. The primary amine adjacent to $E_N$ made availiable for N-terminal protein sequencing after N−S acyl rearrangement is denoted with an asterisk. Letters identifying distinct species are as in eqs 1−4. Although spontaneous N-terminal cleavage can occur via hydrolysis of either the linear or branched thioester intermediates, only the major pathway (V) is shown.

addition to these requisite intein residues, a nucleophilic residue (Ser/Thr/Cys) at the first C-extein position (the $^{+}1$ residue) is required for splicing activity (*5*, *21*, *22*, *28*−*30*). Detection of a zinc ion chelated to the Cys$^{+}1$ residue in the X-ray crystallographic structure of the *Saccharomyces cerevisiae* VMA intein (*26*) encouraged investigations into the effects of divalent metal cations on intein activity. In vitro, the addition of $Zn^{2+}$ to both the *Mtu* RecA and *Ssp* DnaE inteins decreased the extent of splicing detected after overnight incubation (*31*, *32*). Inhibition of induced N-terminal cleavage was also detected, and both effects were reversed by overnight incubation with EDTA (*31*, *32*). Interestingly, substitution of the *Mtu* RecA Cys$^{+}1$ residue with alanine did not weaken the inhibitory effects of $Zn^{2+}$ on N-terminal cleavage (*32*), whereas the identical substitution in the *Ssp* DnaE intein resulted in a cleavage-deficient intein, precluding further analysis (*31*).

The naturally split *Ssp* DnaE intein has proven to be a useful and powerful model for the study of intein kinetics (*18*). This is the first study to examine the effects of an inhibitor on the kinetics of intein-mediated reactions. We identify specific reaction steps inhibited by $Zn^{2+}$ and describe reaction intermediates not previously reported for the naturally split *Ssp* DnaE intein. These intermediates provide direct evidence of intein association. Previously, contributions of the spontaneous hydrolysis and trans splicing reactions to the observed kinetics of induced reactions (e.g., DTT-induced N-terminal cleavage) could not be discerned. Through this comparative kinetic study employing both site-directed mutagenesis at the Cys$^{+}1$ residue and $Zn^{2+}$-mediated reaction inhibition, we describe herein the maximum contribution of the spontaneous cleavage process to overall cleavage kinetics, identify the major pathway of the hydrolysis reaction, and demonstrate its inhibition. The stepwise control of products through the trans cleavage pathway using $Zn^{2+}$ and EDTA is also addressed.

## MATERIALS AND METHODS

*Strains and Constructs.* Plasmids pMEB2 and pMETXB1 have been described previously (*13*, *18*). pMEB2 encodes a

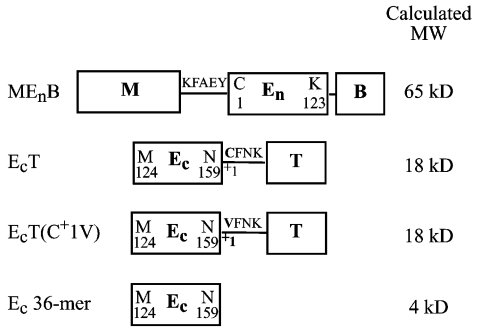


FIGURE 2: Diagram of fusion proteins and synthetic peptides. Experiments described herein employed the two domains of the *Ssp* DnaE intein purified separately as fusion proteins [$ME_nB$, $E_cT$, and $E_cT(C^+1V)$] or synthesized as a peptide ($E_c$ 36-mer). Thioredoxin (T, ~14 kDa) and the maltose binding protein (M, ~43 kDa) of *E. coli* and the *B. circulans* chitin binding domain (B, ~7 kDa) flanked the *Ssp* DnaE intein N- or C-terminal domain ($E_n$ or $E_c$, respectively). Native extein residues KFAEY and CFNK were included at the intein N- and C-termini, as indicated. A synthetic peptide was designed to match the sequence of $E_c$ without C-extein residues. Calculated molecular masses are indicated to the right of each construct for comparison.

fusion protein consisting of the *E. coli* maltose binding protein (MBP, or M), the N-terminal portion of the *Synechocystis* sp. PCC6803 (*Ssp*) DnaE intein ($E_n$) preceded by five native N-terminal extein residues (KFAEY), and the *Bacillus circulans* chitin binding domain (CBD, or B) all under control of an IPTG inducible tac promoter (Figure 2). pMETXB1 encodes a fusion protein consisting of the *Ssp* DnaE intein C-terminal domain ($E_c$), four native extein residues (CFNK), *E. coli* thioredoxin (Trx, or T), the *Mycobacterium xenopi* GyrA intein containing an asparagine 198 to alanine substitution, and the CBD under control of an IPTG inducible T7 promoter. The codon for the first C-extein residue following the *Ssp* DnaE intein was mutated to encode valine ($C^+1V$) by polymerase chain reaction using the following forward and reverse primers: 5′-CTGCTAGCCAACGGCGCTATCGCTGCTAAC**GTG**-TTTAACAAAAATTGTGGTGG-3′ (valine codon in bold letters) and 5′-GATGCACTAGTTGCCCT-3′, respectively. The resulting plasmid, pMETXB4, was verified by DNA sequencing. *E. coli* strains ER1992 [*D(argF-lac)U169 glnV44 mcr-67 endA1dinD2::MudI1734 (KanR, lacZ$^+$) thi-1D(mcrC-mrr)114::IS10*] and ER2566 [*fhuA2 lacZ::T7 gene1 [lon] ompT gal sulA11 [dcm] R(zgb-210::Tn10-TetS) endA1 D-(mcrC-mrr)114::IS10 R(mcr-73::miniTn10-TetS)2*] were used for plasmid and protein purifications, respectively [New England Biolabs (NEB)].

*Protein Purification*. The fusion protein $ME_nB$ (Figure 2) was expressed and purified from the pMEB2 plasmid as reported previously (*18*). $ME_nB$ protein was eluted from an amylose column equilibrated in buffer A [20 mM Tris (pH 7.0) and 500 mM NaCl] by addition of buffer B [20 mM Tris (pH 7.0), 500 mM NaCl, and 10 mM maltose]. The $E_cT$ fusion protein (Figure 2) was purified as published previously from the pMETXB1 plasmid (*18*). Briefly, $E_cT$ was expressed as a fusion protein with the *Mxe* GyrA intein and chitin binding domain. The four-part fusion was bound to a chitin column in buffer C [20 mM Tris (pH 8.0) and 500 mM NaCl]. Incubation with buffer D [20 mM Tris (pH 7.0), 500 mM NaCl, and 30 mM DTT] initiated cleavage N-terminal of the *Mxe* GyrA intein, allowing elution of the $E_cT$ protein. $E_cT(C^+1V)$ protein was purified similarly from the pMETXB4 plasmid. After purification, $E_cT$ and $E_cT(C^+1V)$ were dialyzed against buffer C to remove DTT and concentrated using an Amicon Centriprep-10 (Millipore Corp.). All protein concentrations were determined by a Bradford assay (Bio-Rad Laboratories, Inc.) using BSA as a standard. Preparation purity was assessed as >90% by PAGE examination. Purified samples were aliquoted, stored at −80 °C, and used immediately after thawing at 4 °C. All buffers and stock solutions were prepared with ultrapure MilliQ water.

The 36-mer peptide matching the sequence of $E_c$ was synthesized (NEB) as described previously (*23*). Stocks of 10 mg/mL peptide were aliquoted, frozen at −20 °C, and used immediately after being thawed at room temperature.

*In Vitro N- and C-Terminal Trans Cleavage Reactions*. N- and C-terminal intein cleavage reactions were examined on the basis of a method described previously (*18*). Specifically, $ME_nB$ and $E_cT$ proteins were incubated at room temperature in buffer A either at equimolar concentrations (12 $\mu$M) or at a 1:3 ratio with excess $E_cT$ protein or $E_c$ peptide (36 $\mu$M). Trans cleavage was induced with either 50 mM DTT or 0.5 M HA (pH 7.0). All cleavage time courses commenced upon addition of the nucleophile to the reaction mixture. Typically, reaction aliquots were removed at intervals up to 24 h later, quenched by dilution into $^1/_3$ volume of 3× SDS sample buffer containing DTT (NEB), and incubated for 30 min at room temperature before being transferred to 4 °C to await electrophoresis. Where indicated, aliquots were boiled or incubated in an 80 °C heating block for 5 min in sample buffer in lieu of room-temperature incubation. Effects of quenching conditions were examined by excluding DTT, SDS, or both from the sample buffer or including TCEP as an alternate reducing agent. Solutions of $ZnCl_2$, $MgCl_2$, $CaCl_2$, or EDTA disodium salt, dissolved in ultrapure MilliQ water, were added to the reaction mixtures immediately prior to DTT or HA addition, unless noted otherwise.

Preincubation experiments were conducted by incubating the intein halves together at room temperature for 20 min prior to DTT addition. Where indicated, $ZnCl_2$ was added either at the beginning (immediately after the intein halves) or at the end (immediately prior to DTT addition) of the 20 min preincubation. Zero points were taken before and after preincubation with the second zero point used to account for effects of the spontaneous trans cleavage process.

*In Vitro Trans Splicing Reactions.* Splicing reactions were conducted by the incubation of $ME_nB$ and $E_cT$ (or $E_c$) at room temperature in buffer A at either a 1:1 or 1:3 molar protein ratio (12−36 $\mu$M) in the absence of DTT or any other exogenous nucleophile. The time course was started upon addition of the C-terminal intein domain to the reaction mixture containing the N-terminal intein domain. Splicing was typically monitored for 24 h, but longer incubations (up to 48 h) were performed if the reaction had not reached a plateau. Reaction aliquots were quenched by dilution into 3× SDS sample buffer and incubated at room temperature for 30 min as described for cleavage experiments. Trans splicing experiments conducted for the $Zn^{2+}$ inhibition curve were conducted at equal molar concentrations (12 $\mu$M) of N- and C-terminal intein domains.

*Data Acquisition.* Quenched samples taken during trans splicing or trans cleavage reactions were equilibrated to room

temperature before being loaded onto Novex 10−20% tricine gels (Invitrogen). After electrophoresis, bands were visualized by Coomassie Blue R250 staining. Protein fusions $ME_nB$ and $E_cT$ migrated with apparent masses of 65 and 18 kDa, respectively, in this system and were easily distinguished from both trans cleavage and trans splicing products. Trans cleavage was monitored by the formation of the N-terminal cleavage product, M, with a mobility of approximately 43 kDa, and C-terminal cleavage product, T, at 12 kDa. The splicing product, MT, was visible at ~57 kDa. Band identities were verified by protein sequencing and Western blot analysis. Protein bands were digitized by a flatbed scanner (Microtek), and densitometric analysis was conducted with NIH Image software (http://rsb.info.nih.gov/nih-image/). For comparison, representative experiments were analyzed using a Molecular Dynamics computing densitometer equipped with ImageQuant software. Both methods yielded similar results.

*Kinetic Analysis of Trans Cleavage and Trans Splicing.* The intein reaction mechanism has been described elsewhere (*3*, *21*, *22*, *24*) and can be divided into cleavage and splicing pathways (Figure 1). For the *Ssp* DnaE intein, both activities involve association of the two halves and formation of a linear thioester via an N−S acyl shift of the N-terminal scissile bond, initiated by Cys1 (Figure 1, reactions I and II). Experimentally, association of the two halves has been demonstrated to be a relatively rapid process compared to the overall rate of trans cleavage and trans splicing and does not contribute to the observed rate constant (*18*). For the *Ssp* DnaE intein and the majority of inteins that have been studied, the spontaneous process of N-terminal cleavage can be dramatically enhanced by the addition of DTT, HA, or MESNA (*21*−*23*). Nucleophilic attack of the linear thioester results in the release of the N-extein. The formation of M is used to monitor the rate of N-terminal cleavage ($k_{obs1}$) as described by Figure 1, reaction III, and eq 1.

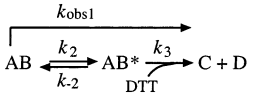


(1)

where AB is the associated intein fusion complex ($ME_nB$−$E_cT$), AB* is the linear thioester intermediate, C is M, and D is the associated $E_nB$:$E_cT$ complex, as identified in Figure 1.

C-Terminal cleavage coupled to succinimide formation results in release of the C-extein from the associated intein complex (Figure 1, reaction IV). For the *Ssp* DnaE intein, there have been no reported conditions under which C-terminal cleavage was detected in the absence of N-terminal cleavage, although these conditions have been described for other inteins (*21*, *22*). The dependence of C-terminal cleavage on upstream reactions has been described previously (*18*) in terms of the observed rate of N-terminal cleavage, $k_{obs1}$, as follows:

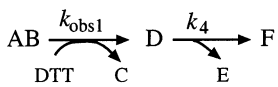


(2)

where E is the C-extein (T) and F is the associated intein complex ($E_nB$:$E_c$).

Alternatively, attack of the linear thioester (AB*) by the nucleophilic $^{+1}$cysteine residue transfers the N-extein to the C-terminus of the intein, yielding a branched thioester intermediate (Figure 1, reaction VI). Succinimide formation by a terminal asparagine residue releases the ligated exteins from the intein (Figure 1, reaction VII). In the final step, uncatalyzed by the intein, the thioester bond joining the two extein sequences is resolved into a peptide bond by an S−N rearrangement (Figure 1, reaction VIII). The rate of trans splicing, $k_{obs2}$ (eq 3), is monitored by the appearance of the spliced product MT.

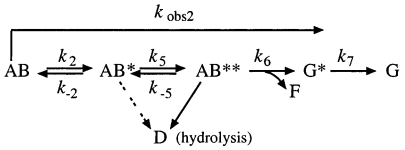


(3)

where AB** is the branched thioester intermediate and G* and G represent the spliced product MT before and after S−N rearrangement, respectively, as identified in Figure 1.

Both N-terminal cleavage and trans splicing processes were treated as first-order, irreversible, pre-steady state reactions and therefore fit to a simple exponential model (Kaleidagraph) described as $P = P_0(1 - e^{-kt})$, where $P$ is the fraction of cleaved or spliced product (M or MT, respectively), $P_0$ is the maximum product formed, $k$ is the observed rate (in inverse seconds), and $t$ is time in seconds (*18*). $P_0$ was allowed to float during fitting. For individual N-terminal cleavage reactions, the fraction of cleaved product, $P$, was derived from the expression $M_n - M_0$ for each given time point, $n$, where $M_0$ represents the amount of M present at the beginning of the reaction. Data (number of replicates, $n \geq 3$) were fit and normalized on the basis of the value for $P_0$ determined by the fitting routine for each individual experiment and averaged to yield the fraction of product formed, $R$, for each condition. Alternate calculations of $P$ to address any loading discrepancies [including ($M_n$/$ME_nB_0$), $M_n$/($M_n$ + $ME_nB_n$), or ($M_n$/total$_n$), where $ME_nB_0$ represents the initial amount of the $ME_nB$ reactant present at time zero and total$_n$ represents the sum of all band densities present at a given time point] had no significant effect on the calculation of $k_{obs1}$ given that $P_0$ was treated as a variable. For preincubated cleavage reactions, $P$ was calculated as the fraction of N-terminal cleavage postincubation by subtracting from each time point $n$ the amount of cleavage that occurred during the incubation ($M_p$) as $M_n - M_p$ prior to data normalization as previously described. The fraction of spliced product (MT) was calculated as MT$_n$/total$_n$, and replicates were normalized and fit as described for N-terminal cleavage data.

For $Zn^{2+}$ inhibition curves, fractional inhibition was calculated as $1 - [k_{obs1(Zn^{2+})}/k_{obs1}]$ for N-terminal cleavage reactions and as $1 - [k_{obs2(Zn^{2+})}/k_{obs2}]$ for trans splicing reactions, where $k_{obs1}$ and $k_{obs1(Zn^{2+})}$ represent the rates of DTT-induced N-terminal trans cleavage in the absence and presence of $ZnCl_2$, respectively. Rates of the trans splicing reaction in the absence and presence of $ZnCl_2$ are represented by $k_{obs2}$ and $k_{obs2(Zn^{2+})}$, respectively.

The process of C-terminal cleavage was treated as an irreversible consecutive reaction with respect to its dependence on N-terminal cleavage as described previously (*18*),

according to eq 4.

$$[E] = AB_0\left[1 + \frac{1}{k_{obs1} - k_4}(k_4 e^{-k_{obs1}t} - k_{obs1} e^{-k_4 t})\right] \quad (4)$$

where $AB_0$ represents the starting concentration of the associated intein halves as defined by the concentration of the limiting domain.

*Identification of Unknown Protein Bands by N-Terminal Sequencing and Western Blot Analysis*. Samples from kinetic experiments were electrophoresed on Novex 10−20% tricine gels as described in Data Acquisition. For N-terminal sequencing, protein bands were subsequently transferred to a PVDF membrane (Problott, Applied Biosystems Inc.) according to the procedure of Matsudaira (*33*), with previously described modifications (*34*). The membrane was stained with Coomassie Blue R250, and desired bands were excised from the surrounding membrane and subjected to sequential degradation on a Procise 494 protein/peptide sequencer (Applied Biosystems Inc.) (*34*). For Western blot analysis, protein bands were transferred to 0.45 $\mu$M nitrocellulose membranes (Schleicher & Schuell) before being probed with one of three primary antibodies against either M (rabbit polyclonal, NEB), B (mouse monoclonal, NEB), or T (mouse monoclonal, Research Diagnostics, Inc.). HRP-conjugated anti-mouse or anti-rabbit secondary antibodies allowed the use of a chemiluminescent detection system for visualization (LumiGlow, Cell Signaling Technology Inc.).

## RESULTS

*Identification of Cleavage and Splicing Intermediates*. The $ME_nB-E_cT$ constructs allow examination of both the starting materials and end products of trans cleavage and splicing reactions by standard protein electrophoresis. Reaction components (starting materials $E_cT$ and $ME_nB$, N-terminal cleavage products M and $E_nB$, C-terminal cleavage products $E_c$ and T, and splicing product MT) are visualized as protein bands with unique mobilities and have been identified by both Western blotting experiments and N-terminal protein sequencing (*13*, *18*). Five additional bands (Figure 3A,C, bands I−V), whose presence following typical sample treatment conditions was both inconsistent and infrequent, were investigated as potential reaction intermediates.

Bands I and II were detected primarily during native trans cleavage reactions, and decreased $E_nB$ and $E_cT$ intensities typically coincided with their presence (Figure 3A, compare lanes 8 and 10). Band I migrated with an apparent mass of 35 kDa, and band II migrated slightly more slowly than the previously identified $E_nB$ protein band, creating the appearance of a doublet at ~25 kDa. Quenching conditions, including temperature, reducing agent, and incubation time, were varied between identical aliquots taken at single time points from native $ME_nB-E_cT$ cleavage reactions. Results from a typical experiment (Figure 3B) illustrate the sensitivity of both the 35 and 25 kDa bands to temperature but not to reducing agent. Neither band could be consistently detected under any conditions that included 5 min of boiling as part of the quenching protocol (lanes 7−9). Incubation at either room temperature (lanes 1−4) or 80 °C (lanes 5 and 6) allowed the formation of bands I and II with increased levels detected at the lower temperature. In contrast, the lower band of the 23−25 kDa doublet, previously identified by N-terminal sequencing as the $E_nB$ fusion protein (the result of N-terminal cleavage of M from the $ME_nB$ starting construct), was present after higher-temperature incubations, either 80 °C or boiling.

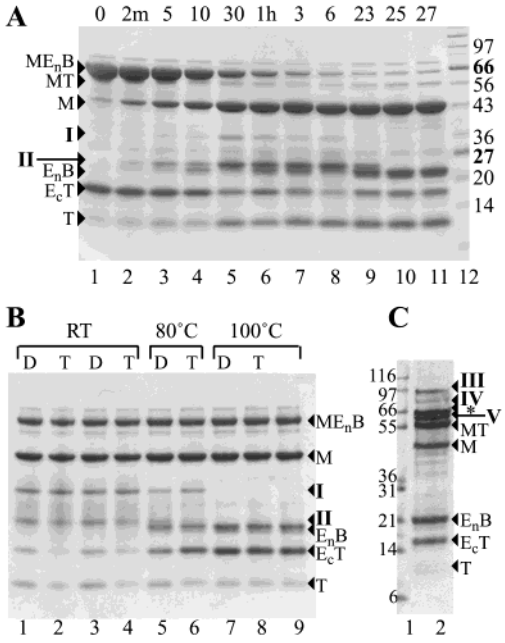


FIGURE 3: Characterization of unknown protein bands detected during trans cleavage and splicing reactions. Reactions were conducted at room temperature with 12 $\mu$M $ME_nB$ and 36 $\mu$M $E_cT$ proteins. Samples were visualized by electrophoresis on 10−20% tricine gels and subsequently stained with Coomassie Brilliant Blue R250. Molecular mass protein markers are in units of kilodaltons. Abbreviations: M, maltose binding protein; $E_n$ and $E_c$, N- and C-terminal halves of the *Ssp* DnaE intein, respectively; T, thioredoxin; B, chitin binding domain. (A) Samples taken from a trans cleavage reaction (containing 50 mM DTT) at the times indicated above each lane were denatured in boiling DTT-containing SDS buffer for 5 min before electrophoresis. (B) Effect of sample treatment conditions on the presence of bands I and II during a trans cleavage experiment. Molecular mass markers are identical to those in panel A. Samples were denatured in buffer containing DTT (lanes 1, 3, 5, and 7) or TCEP (lanes 2, 4, 6, and 8) at room temperature (lanes 1−4), 80 °C (lanes 5 and 6), or 100 °C (lanes 7−9). Incubation times of 5 min (lanes 1, 2, and 5−9) or 30 min (lanes 3 and 4) were used. No additional reducing agent was added to the sample in lane 9. (C) A sample taken at 24 h from a trans splicing reaction mixture was denatured at room temperature for 30 min in DTT-containing SDS buffer before electrophoresis and demonstrates the presence of high-molecular mass intermediates III−V. The asterisk denotes starting material $ME_nB$.

N-Terminal amino acid sequencing results (Table 1) revealed the presence of both $E_n$ and $E_c$ sequence (approximately 1:1) in both the 35 and 25 kDa bands. Western blot analysis determined that neither band was recognized by anti-M Ab, both bands reacted to anti-B Ab, and only the 35 kDa band reacted to anti-T Ab (data not shown). The presence of $E_n$ and $E_c$ sequence and reactivity to anti-B and T Abs identified the 35 kDa protein band as a complex containing the $E_nB$ and $E_cT$ fusion proteins after N-terminal cleavage (represented herein as $E_nB$:$E_cT$). The 25 kDa band with both $E_c$ and $E_n$ sequence and reactivity only to anti-B Ab was therefore identified as the $E_nB$:$E_c$ complex (the 35 kDa complex after C-terminal cleavage). These complexes were resolved into their component bands ($E_nB$, $E_cT$, and $E_c$) upon boiling. These data are consistent with the molecular mass of each component and suggest that fusion protein

Table 1: Results of N-Terminal Amino Acid Sequencing for Bands I−V Compared to Known Sequence of the N-Termini[a] of M, $E_n$, and $E_c$

| Band | MW[b] | Sequencing Results | | | | | | | | | | | | | | Identity[c] |
|---|---|---|---|---|---|---|---|---|---|---|---|---|---|---|---|---|
| | | 1 | 2 | 3 | 4 | 5 | 6 | 7 | 8 | 9 | 10 | 11 | 12 | 13 | 14 | |
| I | 35 kD | C | L | S | F | | T | E | I | | T | | E | Y | G | $E_nB$:$E_cT$ |
| | | | | | | **G** | | | | **L** | | **V** | | | | |
| | | V | K | V | I | | R | R | S | | G | | Q | R | I | |
| II | 25 kD | | L | S | F | | T | E | I | | T | | | | | $E_nB$:$E_c$ |
| | | | | | | **G** | | | | **L** | | | | | | |
| | | V | K | V | I | | R | R | S | | G | | | | | |
| III | 95 kD | | L | S | F | | T | E | I | | T | | | Y | **G** | M-$E_nB$:$E_cT$ |
| | | | | | | **G** | | | | **L** | | **V** | | | | |
| | | V | | V | I | | | | | | | | Q | R | I | Or |
| | | | **K** | | | | | | | | | | | | | |
| | | M | | T | E | E | | K | L | V | I | W | I | N | **G** | $E_nB$:$E_cT$-M |
| IV | 83 kD | | L | | F | | T | E | I | | T | | | | | M-$E_nB$:$E_cT$ |
| | | | | | | **G** | | | | **L** | | | | | | |
| | | V | | V | I | | R | R | S | | | | | | | Or |
| | | | **K** | | | | | | | | | | | | | |
| | | | | T | E | E | | K | L | V | I | | | | | $E_nB$:$E_cT$-M |
| V | 60 kD | V | | | I | | R | R | S | | | V | Q | | | $E_cT$-M |
| | | | **K** | | | | | | | | | | | | | |
| | | M | | T | E | E | G | K | L | V | I | W | I | N | G | |
| I*[d] | 35 kD | | L | S | F | | T | E | I | | T | | E | Y | G | $E_nB$:$E_cT$ |
| | | | | | | **G** | | | | **L** | | **V** | | | | |
| | | V | K | V | I | | R | R | S | | G | | Q | R | I | |
| | | C | L | S | F | G | T | E | I | L | T | V | E | Y | G | **$E_n$** |
| | | V | K | V | I | G | R | R | S | L | G | V | Q | R | I | **$E_c$**[e] |
| | | M | K | T | E | E | G | K | L | V | I | W | I | N | G | **M** |

[a] Each column of sequence (presented in the conventional one-letter amino acid code) represents results from one round of sequencing. Results within each column are organized for comparison to known sequences presented at the bottom of the table. At least 10 rounds of sequencing were performed on each sample. Results in bold indicate sequence positions at which the proteins represented above and below the letter share identical amino acid residues. [b] Molecular masses were estimated from protein gel electrophoresis by comparison to a broad range protein marker (NEB). [c] Band identification relied on sequencing results, electrophoretic mobility, and Western blot experiments. Covalent interactions are represented with a dash and noncovalent interactions (i.e., association) with a colon. [d] Band I* was isolated from a trans cleavage experiment conducted in the presence of 1 mM $ZnCl_2$. [e] N-Terminal sequencing determined that the starting methionine of the Ec sequence is processed by *E. coli* and is therefore not shown.

mobility is not altered significantly by complex formation. Because intermediates provide crucial information about reaction progression, samples described in this study were incubated at room temperature for 30 min, in 3× SDS buffer containing DTT (as described in Materials and Methods) unless indicated otherwise.

Characterization of bands III−V (Figure 3C, lane 2) was also undertaken. Sample treatment conditions were again varied, and bands IV and V were more frequently detected in samples from experiments lacking DTT than those containing the nucleophile. However, the consistent visualization of bands III−V was not achieved, suggesting their increased sensitivity to denaturing conditions. N-Terminal amino acid sequencing demonstrated the presence of multiple N-termini in each of these high-molecular mass bands (Table 1). Sequence consistent with the N-termini of $E_n$, $E_c$, and M proteins was detected in bands III and IV. Both $E_c$ and M sequence could be detected in band V. Because linear thioester formation makes a primary amine at the N-terminus available for N-terminal sequencing (Figure 1, asterisk), both the linear and the branched thioester were expected to yield identical sequencing results (i.e., the presence of M, $E_n$, and $E_c$ sequence). Bands III and IV were therefore identified as the associated linear and branched thioester intermediates (M−$E_n$B:$E_c$T and $E_n$B:$E_c$T−M). However, these isomers could not be uniquely identified by N-terminal sequencing alone. Band IV electrophoretic mobility was consistent with the molecular mass of the associated species (approximately 83 kDa), whereas band III migrated more slowly (Figure 3C). An anomalous electrophoretic mobility has been reported for the branched thioester intermediate of full-length intein reactions (*4*, *21*, *22*), suggesting that band III may be the associated branched thioester of the *Ssp* DnaE intein. The faster mobility and two N-termini imply that band V is the branched thioester in its dissociated form ($E_c$T-M). Examination of the previously identified reaction bands (e.g., M and $E_c$T) failed to detect the presence of more than one N-terminus in any sample (data not shown).

*Effects of $ZnCl_2$ and $^+$1 Substitution on N-Terminal Trans Cleavage.* An examination of both N- and C-terminal trans cleavage rates in the presence and absence of 1 mM $ZnCl_2$ was undertaken with both the native $E_c$T and mutant $E_c$T($C^+$1V) proteins. In the absence of $ZnCl_2$, N-terminal cleavage experiments yielded a $k_{obs1}$ of $(1.6 \pm 0.1) \times 10^{-3}$ $s^{-1}$ ($n = 7$), similar to that published previously (*18*). The addition of 1 mM $ZnCl_2$ at the start of the time course had a minor effect [3-fold inhibition, $k_{obs1(Zn^{2+})} = (0.5 \pm 0.04) \times 10^{-3}$ $s^{-1}$ ($n = 4$), Figure 4] on the N-terminal cleavage activity of the $ME_nB-E_cT$ proteins. Because maximum cleavage (~80% of starting material $ME_nB$) was still reached within the 24 h time frame of the experiments (compare panels A and B of Figure 4, lane 10), comparison of cleavage extents after overnight incubation would be insufficient to detect inhibition. The rate of N-terminal cleavage was not decreased by the addition of either 1 mM $MgCl_2$ or 1 mM $CaCl_2$ (data not shown). To verify that DTT did not interfere with interpretation of $Zn^{2+}$ studies, control experiments were conducted using hydroxylamine (HA) to induce trans cleavage. Results were similar to those employing DTT to induce cleavage. In both the absence and presence of 1 mM $ZnCl_2$, maximum cleavage extents were reached prior to the 24 h time point (data not shown). These data suggest that the inability of $ZnCl_2$ to completely inhibit the N-terminal cleavage reaction cannot be explained by a competing DTT−$Zn^{2+}$ interaction.

Substituting the $Cys^+$1 residue of $E_c$T with valine alleviated the $ZnCl_2$ effect on N-terminal cleavage, yielding similar rate constants of $(0.11 \pm 0.01) \times 10^{-3}$ and $(0.09 \pm 0.01) \times 10^{-3}$ $s^{-1}$, in the absence and presence, respectively, of 1.0 mM $ZnCl_2$ (Figure 5). This result supports the view of the $^+$1 cysteine residue as a $Zn^{2+}$ chelator (*26*, *31*). Despite the ability of the $C^+$1V mutation to abrogate $ZnCl_2$ effects on N-terminal cleavage, the mutant also displayed significantly altered kinetics in comparison to the native sequence (Figure 5C, inset). The rate of native $ME_nB-E_cT$ N-terminal cleavage [$(1.6 \pm 0.1) \times 10^{-3}$ $s^{-1}$] was significantly faster than that calculated for the valine mutant [$(0.11 \pm 0.01) \times 10^{-3}$ $s^{-1}$]. Interestingly, both previous and current experiments with a 36-mer $E_c$ peptide devoid of any C-terminal extein sequence have demonstrated that the $^+$1 residue is not required for N-terminal cleavage (*18*).

*Effect of $ZnCl_2$ and $^+$1 Substitution on C-Terminal Trans Cleavage.* Whereas N-terminal cleavage was slowed approximately 3-fold in the presence of 1 mM $ZnCl_2$, C-terminal cleavage was more dramatically inhibited. Only

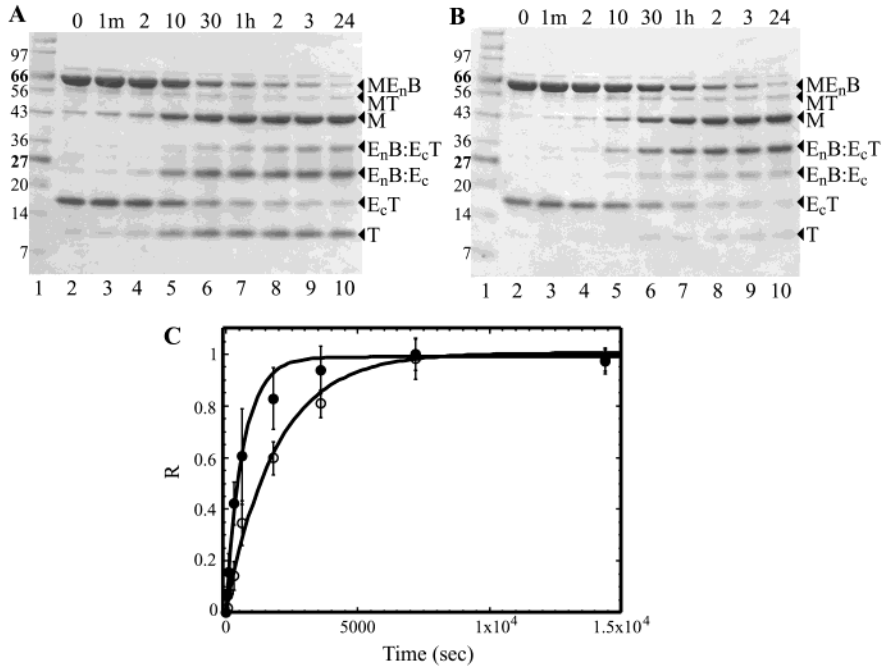


FIGURE 4: Effects of $ZnCl_2$ on native N-terminal trans cleavage reactions. Cleavage time courses commenced upon addition of 50 mM DTT. Samples from trans cleavage experiments conducted with 12 $\mu$M $ME_nB$ and 36 $\mu$M $E_cT$ in the absence (A) or presence (B) of 1 mM $ZnCl_2$ were denatured at room temperature for 30 min in DTT-containing SDS buffer before electrophoresis on 10−20% tricine gels. Abbreviations are as in the legend of Figure 3 and protein standard molecular masses (lane 1) are expressed in kilodaltons. Time points are indicated above each lane. (C) Fraction of N-terminal cleavage (R) as a function of time in the presence (○) or absence (●) of 1 mM $ZnCl_2$ from four to eight individual experiments, including those depicted in panels A and B. Solid lines represent the fit of each data set to the relation $P = P_0(1 - e^{-kt})$, and error bars signify the standard deviation of the data obtained at each time point.

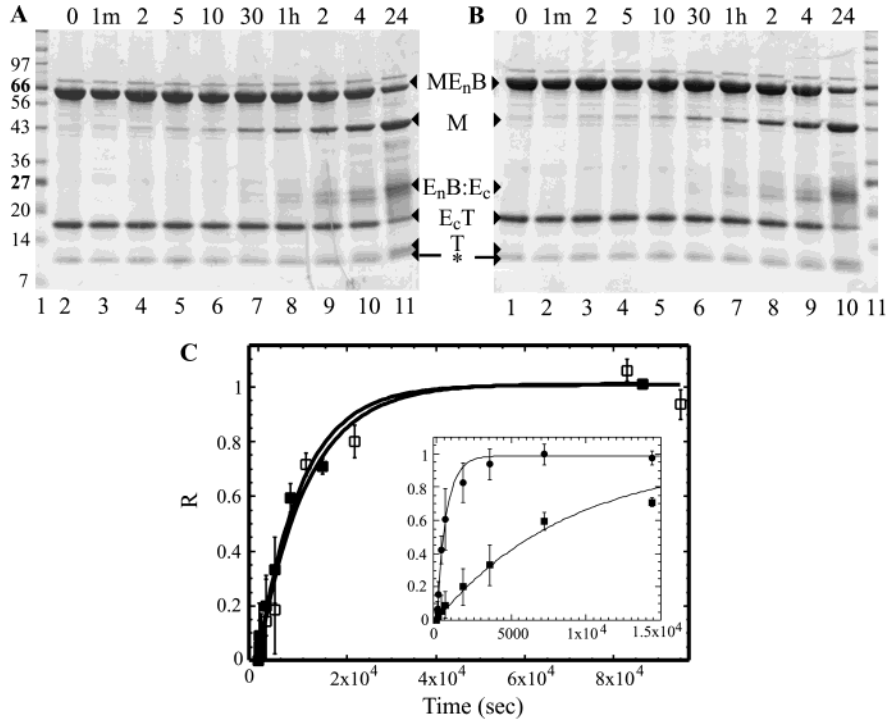


FIGURE 5: Analysis of $ZnCl_2$ effects on the N-terminal trans cleavage activity of the $C^+1V$ mutant. Conditions for the $ME_nB-E_cT(C^+1V)$ trans cleavage reactions and sample treatment are as described in the legend of Figure 4. Experiments were conducted in the absence (A) or presence (B) of 1 mM $ZnCl_2$. Molecular mass protein standards are expressed in kilodaltons. Time points are indicated above each lane. The asterisk identifies a low-molecular mass contaminant in the preparation. (C) Fraction of N-terminal cleavage (R) as a function of time in the presence (□) and absence (■) of 1 mM $ZnCl_2$. The inset provides direct comparison of N-terminal cleavage data in the absence of $Zn^{2+}$ from the valine mutant (■) to that of the native $^+1$ cysteine residue (●). Solid lines represent the fit of each data set ($n \geq 3$, and includes experiments represented in panels A and B) to $P = P_0(1 - e^{-kt})$, and error bars demonstrate the standard deviation of the data obtained at each time point.

minor amounts of product T were visible even at the latest time points, suggesting that $Zn^{2+}$ effectively inhibits the C-terminal cleavage reaction (Figure 4A,B). The faint nature of the T band precluded an accurate kinetic quantitation of

C-terminal cleavage in the presence of $ZnCl_2$. As described for N-terminal cleavage, the addition of 1 mM $MgCl_2$ or $CaCl_2$ did not inhibit the kinetics of C-terminal cleavage. Interestingly, substitution of the $^{+}1$ cysteine for valine did not completely abrogate C-terminal cleavage, with similar cleavage extents observed in either the absence or presence of $ZnCl_2$ (Figure 5A,B). Thorough quantitation of cleavage rates was restricted by the faint nature of the T band and the presence of a low-molecular mass contaminant in the mutant protein preparation (Figure 5, asterisk).

Whereas thioredoxin band intensity was markedly decreased during $ME_nB-E_cT$ cleavage experiments that included $ZnCl_2$, the intensity of the 35 kDa band (the $E_nB$:$E_cT$ protein complex) was consistently increased (compare panels A and B of Figure 4, lanes 6−10). Accumulation of this intermediate would occur if $Zn^{2+}$-mediated inhibition of C-terminal cleavage prevented resolution of the complex into $E_nB$:$E_c$ (25 kDa band) and T (14 kDa band) components. Alternatively, $Zn^{2+}$ chelation of intein residue(s) could lead to stabilization of the associated complex even after C-terminal cleavage, effectively "trapping" thioredoxin in the complex (i.e., $E_nB$:$E_c$ and T present in the 35 kDa band). N-Terminal protein sequencing of the 35 kDa band accumulated in the presence of $ZnCl_2$ confirmed both the absence of free T sequence and the presence of $E_n$ and $E_c$ sequence in an approximate 1:1 ratio (Table 1, band I*), verifying the components of the intermediate and supporting the former hypothesis.

*Preincubation Studies of Trans Cleavage in the Presence and Absence of $ZnCl_2$.* The concentration of the two main intein reaction components (intein and extein) cannot be varied with respect to each other, precluding analysis of intein kinetics by typical bimolecular rate equations. Instead, preincubation studies have been used to gain insight into *Ssp* DnaE reaction kinetics. Preincubation of the two *Ssp* DnaE intein domains for up to 90 min prior to DTT addition has no effect on the rate of either N- or C-terminal trans cleavage (*18*). These data were used as evidence for the rapid association of the intein halves relative to the rate of the entire cleavage process (*18*) but also suggest the lack of a rate-limiting step upstream of nucleophilic thioester attack (Figure 1, reaction III). A similar preincubation study was employed in this work to determine whether the reaction step(s) affected by $ZnCl_2$ could be identified. Preincubation experiments would result in an increased rate of N-terminal cleavage if $Zn^{2+}$ acts by retarding a step prior to DTT-mediated thioester attack. Experiments were conducted by incubating the two intein halves ($ME_nB$ and $E_cT$) in the presence of 1 mM $ZnCl_2$ for 20 min prior to the addition of DTT. The resulting rate of N-terminal cleavage was not significantly altered by $ZnCl_2$ addition at the beginning of the incubation [$k_{obs1(Zn^{2+})} = (0.53 \pm 0.10) \times 10^{-3}$ s$^{-1}$ ($n$ = 5), Figure 6]. Similar results were obtained upon addition of $ZnCl_2$ after the 20 min incubation [$k_{obs1(Zn^{2+})} = (0.67 \pm 0.19) \times 10^{-3}$ s$^{-1}$ ($n$ = 5), data not shown]. Because preincubated reactions did not proceed faster than their nonincubated counterparts, it is unlikely that either intein association or the N−S acyl shift reaction is inhibited by $Zn^{2+}$. As reported previously (*18*), we report that preincubation alone had no significant effect on the kinetics of native $ME_nB-E_cT$ N-terminal cleavage [$k_{obs1} = (1.5 \pm 0.1) \times 10^{-3}$ s$^{-1}$ ($n$ = 4)]. Neither preincubation alone nor $ZnCl_2$ addition either before or after the 20 min preincubation affected the N-terminal cleavage rate of the valine mutant (data not shown).

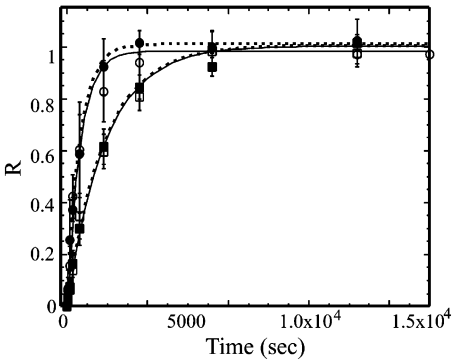


FIGURE 6: Effects of preincubation on N-terminal cleavage kinetics in the presence or absence of $ZnCl_2$. Trans cleavage reaction mixtures containing 12 $\mu$M $ME_nB$ and 36 $\mu$M $E_cT$ were conducted with or without a 20 min incubation prior to the addition of 50 mM DTT. Identical experiments were conducted in the presence of 1 mM $ZnCl_2$. Data are presented as the average of all identical reaction replicates ($n$ = 4−7), and were graphed and fit as described in the legend of Figure 5. Error bars represent one standard deviation. Data symbols and fit lines represent experiments with (filled symbols, dashed lines) or without (empty symbols, solid lines) a preincubation step conducted in the presence (squares) or absence (circles) of 1 mM $ZnCl_2$.

*EDTA Reversal of $ZnCl_2$ Inhibition.* $Zn^{2+}$ has been reported to be copurified with a mutant of the *Sce* VMA1 intein (*26*). To examine whether $Zn^{2+}$ had been copurified with the *Ssp* DnaE intein domains, we examined the ability of the split intein to undergo trans cleavage and splicing in the presence of 2 mM EDTA. EDTA is known to reverse intein inhibition by zinc ion (*31*, *32*). Reaction rates were similar in either the presence or absence of the chelator, demonstrating the lack of any inhibitory metal in the protein preparations (data not shown). Interestingly, the addition of EDTA to cleavage reaction mixtures that included $ZnCl_2$ allowed stepwise control of the C-terminal cleavage reaction. Cleavage reactions were allowed to proceed in the presence of 1 mM $ZnCl_2$ from 1 to 24 h before the addition of 2 mM EDTA. Aliquots taken from the reaction mixture before and after EDTA addition were incubated at room temperature to prevent dissociation of the intermediate complexes. Figure 7 documents a representative experiment in which 1 mM $ZnCl_2$ was added at the commencement of the cleavage reaction and 2 mM EDTA was added immediately after the 1 h time point. Prior to EDTA addition, typical $ZnCl_2$ effects were observed, including the intense 35 kDa $E_nB-E_cT$ complex and the absence of free T protein (Figure 7, lanes 3−5). However, 10 min after addition of EDTA, the intensity of the 35 kDa complex decreased, and the T protein band became visible (Figure 7, lane 6). Similar experiments have documented the appearance of thioredoxin within 1 min of EDTA addition (data not shown). Because free T protein could not be detected in the 35 kDa complex (Table 1, band I*), we propose that the increase reflects a rapid C-terminal cleavage process, otherwise inhibited by $ZnCl_2$. In the presence of EDTA, C-terminal cleavage reached completion within minutes. A rapid C-terminal cleavage step is consistent with the similarly timed appearance of N- and C-terminal cleavage products detected in the absence of $ZnCl_2$ (Figure 4A). Sample buffer addition in lieu of EDTA had no effect

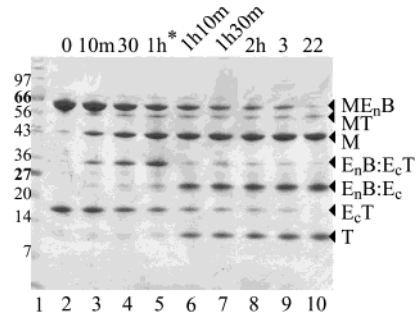


FIGURE 7: Resolution of $ZnCl_2$-accumulated cleavage intermediates by EDTA. Trans cleavage of the $ME_nB-E_cT$ constructs conducted in the presence of 1 mM $ZnCl_2$ proceeded for 1 h before EDTA addition to a final concentration of 2 mM. Samples were treated and visualized as described in the legend of Figure 4. Abbreviations are as in the legend of Figure 3. Noted on the top of each lane is the time that passed from the start of the reaction. EDTA was added immediately after the 1 h time point had been taken (asterisk). Note the rapid increase in the level of the T band upon addition of chelator.

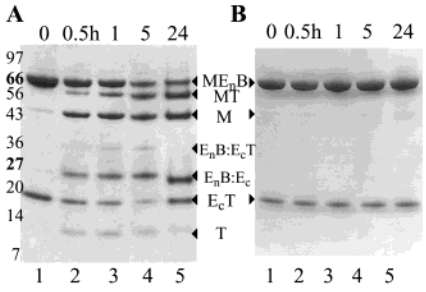


FIGURE 8: Effects of $ZnCl_2$ on $ME_nB-E_cT$ trans splicing and spontaneous hydrolysis reactions. Representative trans splicing experiments in which 12 $\mu$M $ME_nB$ and 36 $\mu$M $E_cT$ were incubated at room temperature in the absence of DTT, in either the absence (A) or presence (B) of 1 mM $ZnCl_2$, are shown. Protein electrophoresis and abbreviations are as described in the legend of Figure 3. Sample treatment conditions are as in Figure 4. The time at which each sample was taken from the reaction mixture and the reaction quenched with SDS buffer is indicated at the top of each lane.

on the presence of either the complex or the T protein band (data not shown).

*Effects of $ZnCl_2$ and $^+1$ Substitution on Trans Splicing.* Given the crucial nature of the $^+1$ sulfhydryl in trans splicing reactions (*5*, *21*, *28*, *30*) and its proposed interaction with $Zn^{2+}$ (*26*, *31*), it was not surprising that 1 mM $ZnCl_2$ was sufficient to inhibit trans splicing reactions of the *Ssp* DnaE intein [Figure 8A,B, $k_{obs2(Zn^{2+})} \leq 1 \times 10^{-6}$ $s^{-1}$]. Similarly, substitution of the native cysteine residue with valine resulted in complete inhibition of trans splicing (data not shown). Notably, a dramatic reduction in both the N- and C-terminal cleavage typically observed during splicing reactions (i.e., spontaneous cleavage) using either the $E_cT$ construct in the presence of $ZnCl_2$ or the $E_cT(C^+1V)$ construct was also detected (Figure 8 and data not shown). The extent of spontaneous cleavage was also significantly reduced during experiments (conducted in the absence of $ZnCl_2$) that employed a synthetic 36-amino acid peptide comprised of the $E_c$ sequence lacking any C-extein residues (data not shown). Both the synthetic 36-mer and the $C^+1V$ mutant undergo DTT-mediated N-terminal cleavage (at dissimilar rates) but lack the crucial nucleophilic $^+1$ residue required for formation of the branched thioester intermediate. These data suggest that the major pathway of spontaneous N-terminal cleavage is via hydrolysis of the branched thioester intermediate and not the linear thioester. The similar profile of $Zn^{2+}$-mediated effects further suggests that the metal inhibits formation of the branched thioester intermediate. Neither 1 mM $CaCl_2$ nor 1 mM $MgCl_2$ was sufficient to inhibit the rate of N- and C-terminal trans cleavage or trans splicing (data not shown). As expected, addition of 1 mM $ZnCl_2$ to the $ME_nB-E_cT(C^+1V)$ reaction mixture had no additional effect (data not shown). Splicing kinetics for the $ME_nB$ and $E_cT$ constructs in the absence of $Zn^{2+}$ have been documented (*18*) and are similar to results from this study [$k_{obs2} = (0.33 \pm 0.04) \times 10^{-3}$ $s^{-1}$].

*Inhibition of Intein-Mediated Reactions as a Function of $ZnCl_2$ Concentration.* To further quantitate the inhibitory effects of $Zn^{2+}$ on intein-mediated reactions, the rates of trans cleavage ($k_{obs1}$) and trans splicing ($k_{obs2}$) were examined at various metal concentrations. The majority of N-terminal cleavage reactions described in this study employed 50 mM DTT as a nucleophile. Because of the potential interaction between zinc ion and the thiol groups of DTT, we sought to verify that the concentration of $ZnCl_2$ used in this study was sufficient to achieve maximum inhibition of the DTT-induced reaction. In the presence of 1 mM $ZnCl_2$, we report a 3-fold inhibition of the rate of N-terminal cleavage in the *Ssp* DnaE intein (see Figure 4C). Further experiments quantitated the rate of N-terminal cleavage in the presence of 0.05−1.5 mM $ZnCl_2$. The results were expressed relative to the rate of trans cleavage in the absence of $ZnCl_2$, to yield the fraction of inhibition as a function of $Zn^{2+}$ concentration. As seen in Figure 9A, concentrations of $ZnCl_2$ from 0.5 to 1.5 mM resulted in a similar level of trans cleavage inhibition, demonstrating a maximum $Zn^{2+}$ effect in the range of 65−75% inhibition.

As described in detail in the legend of Figure 8, the inhibitory effect of 1 mM $ZnCl_2$ on the trans splicing reaction was significant, evidenced by the absence of spliced product MT. Further examination of $Zn^{2+}$-mediated splicing inhibition was conducted using equimolar N- and C-terminal intein domains at a concentration of 12 $\mu$M. The rate of trans splicing was examined in the presence of $ZnCl_2$, from 2.5 to 20 $\mu$M (Figure 9B). Partial inhibition was achieved at 5, 7.5, and 10 $\mu$M $ZnCl_2$, and complete inhibition was reached at concentrations of $\geq$12 $\mu$M $ZnCl_2$. These data suggest a 1:1 ratio of metal ion to intein complex for maximum inhibition of the splicing reaction. The decreased sensitivity of the N-terminal cleavage reaction to micromolar concentrations of $Zn^{2+}$ may be caused by binding of the metal to DTT (present in trans cleavage but absent from trans splicing reaction conditions). This could result in a decreased concentration of free $Zn^{2+}$ in solution. However, as shown in Figure 9A, maximum inhibition of the N-terminal cleavage reaction can still be achieved, verifying that this interaction does not affect the overall conclusions presented herein.

## DISCUSSION

The inability to control the start of a full-length unmodified intein reaction affords little opportunity for detailed kinetic studies of intein-mediated splicing and cleavage. Use of the naturally split *Ssp* DnaE intein allows examination of these reactions in the absence of denaturants commonly required for activity of artificially split inteins (*35*, *36*). Exploiting both amino acid substitution and small molecule-mediated

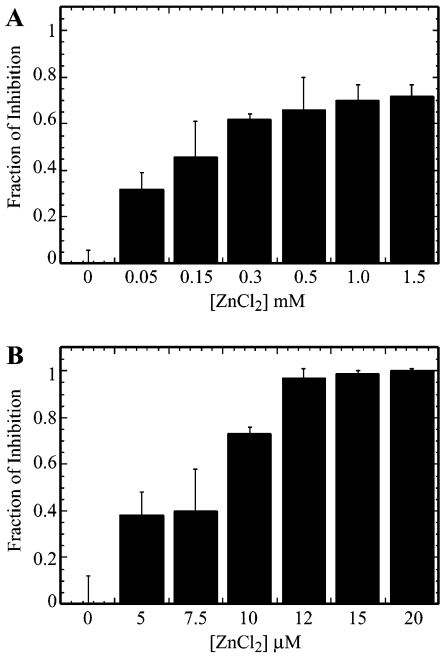


FIGURE 9: Inhibition of the $ME_nB-E_cT$ N-terminal trans cleavage and trans splicing reactions as a function of $ZnCl_2$ concentration. (A) Trans cleavage experiments were conducted at room temperature with 12 $\mu$M $ME_nB$, 36 $\mu$M $E_cT$, 50 mM DTT, and $ZnCl_2$ (concentration ranging from 0.05 to 1.5 mM). Sample treatment and protein electrophoresis conditions were as described in the legend of Figure 4. Resulting values of $k_{obs1(Zn^{2+})}$ were averaged ($n \geq 3$), and error bars reflect the standard deviation under each condition. Individual experiments conducted at each $ZnCl_2$ concentration were fit as described in Materials and Methods. Fractional inhibition of N-terminal cleavage was calculated as $1 - [k_{obs1(Zn^{2+})}/k_{obs1}]$, using the value of $k_{obs1}$ reported herein. A value of 1 represents complete inhibition. (B) Trans splicing experiments were conducted at room temperature with 12 $\mu$M $ME_nB$, 12 $\mu$M $E_cT$, and $ZnCl_2$ (concentration ranging from 2.5 to 20 $\mu$M). Fractional inhibition of splicing was calculated as $1 - [k_{obs2(Zn^{2+})}/k_{obs2}]$, using the value of $k_{obs2}$ reported herein. Analysis is as described for panel A. At least three individual experiments were conducted at each $ZnCl_2$ concentration.

inhibition, we have expanded the understanding of intein kinetics using this previously described model system (*13*, *18*). The presence of complexes representing the associated intein intermediates in the early time points of the reactions (between 1 and 2 min) supports the hypothesis that intein association is rapid relative to overall reaction rates (*18*). Similarities between the kinetics of the *Ssp* DnaE intein reactions and observed reaction rates (or reaction half-times) reported for individual reaction steps of full-length or artificially split inteins (*37*−*40*) continue to validate the use of the naturally split *Ssp* DnaE intein as a general model for the study of intein reaction kinetics.

As was suggested by Mills and Paulus (*32*), the use of $Zn^{2+}$ as a reaction inhibitor has indeed been informative for the study of intein-mediated processes. Both spontaneous (i.e., hydrolysis) and DTT-mediated N-terminal cleavage can potentially contribute to the overall rate of N-terminal cleavage. The inhibition of hydrolysis through amino acid substitution and $ZnCl_2$ addition yields significantly different effects on overall cleavage kinetics (15- and 3-fold inhibition, respectively), suggesting that the 3-fold decrease in the rate of cleavage upon metal addition represents the maximum potential contribution of hydrolysis to the observed rate of N-terminal cleavage. Thus, the $C^+1V$ mutant likely affects both the hydrolysis- and DTT-mediated processes to yield a 15-fold decrease in overall N-terminal cleavage kinetics.

Spontaneous cleavage is believed to result from the hydrolysis of either the branched or linear thioester intermediate (*18*, *21*, *22*). Because hydrolysis- and DTT-mediated cleavage share in common their first two reaction steps (association and N−S acyl shift), it is likely that a downstream step not shared by the two reactions gives rise to the differential inhibition reported in this study. The $^+1$ nucleophile has been demonstrated to be required for formation of the branched but not the linear thioester intermediate (*22*, *41*). Thus, the dramatic inhibition of spontaneous cleavage detected upon removal of the $^+1$ nucleophile (either by substitution with valine or by deletion) suggests that hydrolysis occurs largely via attack of the branched thioester intermediate. The similar inhibition profile observed for the native $ME_nB-E_cT$ constructs upon $ZnCl_2$ addition suggests that $Zn^{2+}$ also affects formation of the branched intermediate. These data lend support to the hypothesis (*31*) that $Zn^{2+}$ inhibition of the *Ssp* DnaE intein acts via chelation of the $^+1$ sulfhydryl.

The use of $ZnCl_2$ to block spontaneous hydrolysis during intein incubation allowed us to demonstrate that the rate of N-terminal cleavage is largely controlled by the rate of thioester attack, and that the steps of association and N−S acyl shift are relatively rapid. Because the magnitude of zinc-mediated inhibition is unaltered whether $ZnCl_2$ is added before or concurrent with DTT, we propose that $Zn^{2+}$ does not inhibit either of these rapid reaction steps. A more thorough understanding of the effect of $Zn^{2+}$ on C-terminal trans cleavage was gained by comparative studies conducted in the presence and absence of EDTA, previously demonstrated to reverse the inhibitory effects of $Zn^{2+}$ in overnight reactions (*31*, *32*). The ability of EDTA to reverse $ZnCl_2$ effects within minutes resulted in the rapid appearance of the C-terminal cleavage product thioredoxin, providing a level of control not exhibited previously for this reaction step.

We have demonstrated that the *Ssp* DnaE intein $C^+1V$ mutant is not sensitive to $Zn^{2+}$-mediated inhibition, supporting the hypothesis (*31*) that $Zn^{2+}$ acts through chelation of the $^+1$ nucleophile. However, a $Cys^+1Ala$ mutant of the *Mtu* RecA intein was demonstrated to retain its sensitivity to $ZnCl_2$ after overnight incubations (*32*). Examination of available structural information from a third intein, the *S. cerevisiae* VMA intein (*26*), revealed three zinc-coordinating residues [Cys455 (the $^+1$ cysteine), Glu80, and His453] in addition to one chelated water molecule. Interestingly, although this histidine residue is typically conserved among inteins, the native *Ssp* DnaE intein contains an alanine at the corresponding (penultimate) position. The presence of a penultimate histidine residue in the *Mtu* RecA intein may allow $Zn^{2+}$ binding and inhibition in the absence of the $^+1$ sulfhydryl. The extra coordination site may also explain the dramatic zinc-mediated inhibition of HA-induced N-terminal cleavage reported for the *Mtu* RecA intein. Upon substitution of the $^+1$ cysteine, the *Ssp* DnaE intein may lack either a sufficient number of coordination sites or a proper conformation to permit $Zn^{2+}$ binding and subsequent inhibition.

We have presented a comparative study designed to examine the detailed roles of individual components in the intein reaction pathways through the use of both amino acid substitution and reaction inhibition. These results represent

the first quantitative examination of intein kinetics in the presence of a known inhibitor. Specific reaction steps inhibited by $Zn^{2+}$ have been described, and reaction intermediates not previously visualized in this system have been identified in this study. These intermediates served not only as reporters of intein association but also as crucial factors in the analysis of intein reaction mechanisms. The use of $Zn^{2+}$ and EDTA can regulate the progression of reactants through the cleavage pathway in a stepwise manner. Finally, amino acid substitution and $Zn^{2+}$ incubation exert differential effects on DTT-mediated N-terminal cleavage and have helped to experimentally define the maximum contribution of hydrolysis-mediated cleavage to the observed rate of N-terminal cleavage. In vivo, inteins execute a unique form of post-translational modification and may be potentially useful in protein regulation. In vitro, inteins have been harnessed for numerous functions in the fields of molecular biology and protein chemistry (reviewed in ref *42*), and both their current and potential future uses will be enhanced by a greater understanding of their activities.

## ACKNOWLEDGMENT

We thank Drs. Ming-Qun Xu, Inca Ghosh, and John S. Olson for valuable discussion, Drs. Lixin Chen, Sharong Chong, Francine Perler, Sriharsa Pradhan, Maurice Southworth, Eric Cantor, and William Jack for critical reading of the manuscript, Ms. Michelle Cushing for technical assistance, and Dr. Donald Comb for support and encouragement.

## REFERENCES

1. Perler, F. B., Davis, E. O., Dean, G. E., Gimble, F. S., Jack, W. E., Neff, N., Noren, C. J., Thorner, J., and Belfort, M. (1994) *Nucleic Acids Res. 22*, 1125−1127.
2. Paulus, H. (2000) *Annu. Rev. Biochem. 69*, 447−496.
3. Noren, C. J., Wang, J., and Perler, F. B. (2000) *Angew. Chem., Int. Ed. 39*, 450−466.
4. Xu, M. Q., Southworth, M. W., Mersha, F. B., Hornstra, L. J., and Perler, F. B. (1993) *Cell 75*, 1371−1377.
5. Cooper, A. A., Chen, Y. J., Lindorfer, M. A., and Stevens, T. H. (1993) *EMBO J. 12*, 2575−2583.
6. Kane, P. M., Yamashiro, C. T., Wolczyk, D. F., Neff, N., Goebl, M., and Stevens, T. H. (1990) *Science 250*, 651−657.
7. Hirata, R., Ohsumk, Y., Nakano, A., Kawasaki, H., Suzuki, K., and Anraku, Y. (1990) *J. Biol. Chem. 265*, 6726−6733.
8. Perler, F. B. (2002) *Nucleic Acids Res. 30*, 383−384.
9. Liu, X. Q. (2000) *Annu. Rev. Genet. 34*, 61−76.
10. Gimble, F. S. (2000) *FEMS Microbiol. Lett. 185*, 99−107.
11. Pietrokovski, S. (2001) *Trends Genet. 17*, 465−472.
12. Telenti, A., Southworth, M., Alcaide, F., Daugelat, S., Jacobs, W. R., Jr., and Perler, F. B. (1997) *J. Bacteriol. 179*, 6378−6382.
13. Evans, T. C., Jr., Martin, D., Kolly, R., Panne, D., Sun, L., Ghosh, I., Chen, L., Benner, J., Liu, X. Q., and Xu, M. Q. (2000) *J. Biol. Chem. 275*, 9091−9094.
14. Derbyshire, V., Wood, D. W., Wu, W., Dansereau, J. T., Dalgaard, J. Z., and Belfort, M. (1997) *Proc. Natl. Acad. Sci. U.S.A. 94*, 11466−11471.
15. Chong, S., and Xu, M. Q. (1997) *J. Biol. Chem. 272*, 15587−15590.
16. Shingledecker, K., Jiang, S. Q., and Paulus, H. (1998) *Gene 207*, 187−195.
17. Lew, B. M., Mills, K. V., and Paulus, H. (1998) *J. Biol. Chem. 273*, 15887−15890.
18. Martin, D. D., Xu, M. Q., and Evans, T. C., Jr. (2001) *Biochemistry 40*, 1393−1402.
19. Wu, H., Hu, Z., and Liu, X. Q. (1998) *Proc. Natl. Acad. Sci. U.S.A. 95*, 9226−9231.
20. Gorbalenya, A. E. (1998) *Nucleic Acids Res. 26*, 1741−1748.
21. Xu, M. Q., and Perler, F. B. (1996) *EMBO J. 15*, 5146−5153.
22. Chong, S., Shao, Y., Paulus, H., Benner, J., Perler, F. B., and Xu, M. Q. (1996) *J. Biol. Chem. 271*, 22159−22168.
23. Evans, T. C., Jr., Benner, J., and Xu, M. Q. (1998) *Protein Sci. 7*, 2256−2264.
24. Paulus, H. (1998) *Chem. Soc. Rev. 27*, 375−386.
25. Klabunde, T., Sharma, S., Telenti, A., Jacobs, W. R., Jr., and Sacchettini, J. C. (1998) *Nat. Struct. Biol. 5*, 31−36.
26. Poland, B. W., Xu, M. Q., and Quiocho, F. A. (2000) *J. Biol. Chem. 275*, 16408−16413.
27. Mizutani, R., Nogami, S., Kawasaki, M., Ohya, Y., Anraku, Y., and Satow, Y. (2002) *J. Mol. Biol. 316*, 919−929.
28. Davis, E. O., Jenner, P. J., Brooks, P. C., Colston, M. J., and Sedgwick, S. G. (1992) *Cell 71*, 201−210.
29. Hodges, R. A., Perler, F. B., Noren, C. J., and Jack, W. E. (1992) *Nucleic Acids Res. 20*, 6153−6157.
30. Hirata, R., and Anraku, Y. (1992) *Biochem. Biophys. Res. Commun. 188*, 40−47.
31. Ghosh, I., Sun, L., and Xu, M. Q. (2001) *J. Biol. Chem. 276*, 24051−24058.
32. Mills, K. V., and Paulus, H. (2001) *J. Biol. Chem. 276*, 10832−10838.
33. Matsudaira, P. (1987) *J. Biol. Chem. 262*, 10035−10038.
34. Waite-Rees, P. A., Keating, C. J., Moran, L. S., Slatko, B. E., Hornstra, L. J., and Benner, J. S. (1991) *J. Bacteriol. 173*, 5207−5219.
35. Southworth, M. W., Adam, E., Panne, D., Byer, R., Kautz, R., and Perler, F. B. (1998) *EMBO J. 17*, 918−926.
36. Mills, K. V., Lew, B. M., Jiang, S., and Paulus, H. (1998) *Proc. Natl. Acad. Sci. U.S.A. 95*, 3543−3548.
37. Chong, S., Williams, K. S., Wotkowicz, C., and Xu, M. Q. (1998) *J. Biol. Chem. 273*, 10567−10577.
38. Southworth, M. W., Amaya, K., Evans, T. C., Xu, M. Q., and Perler, F. B. (1999) *BioTechniques 27*, 110−114, 116, 118−120.
39. Shingledecker, K., Jiang, S., and Paulus, H. (2000) *Arch. Biochem. Biophys. 375*, 138−144.
40. Mootz, H. D., and Muir, T. W. (2002) *J. Am. Chem. Soc. 124*, 9044−9045.
41. Xu, M. Q., Comb, D. G., Paulus, H., Noren, C. J., Shao, Y., and Perler, F. B. (1994) *EMBO J. 13*, 5517−5522.
42. Evans, T. C., Jr., and Xu, M. Q. (1999) *Biopolymers 51*, 333−342.

BI020679E